ACS OMEGA

http://pubs.acs.org/journal/acsodf

Article

Template Removal and Surface Modification of an SSZ-13 Membrane with Heated Sodium Chloride for CO_2/CH_4 Gas Separation

He-Li Wang, Mei-Hua Zhu, Ting Wu, Qin-Liang Jiang, Fei Zhang, Ya-Fen Wu, and Xiang-Shu Chen*

Cite This: *ACS Omega* 2022, 7, 6721−6727

Read Online

ACCESS | Metrics & More | Article Recommendations | Supporting Information

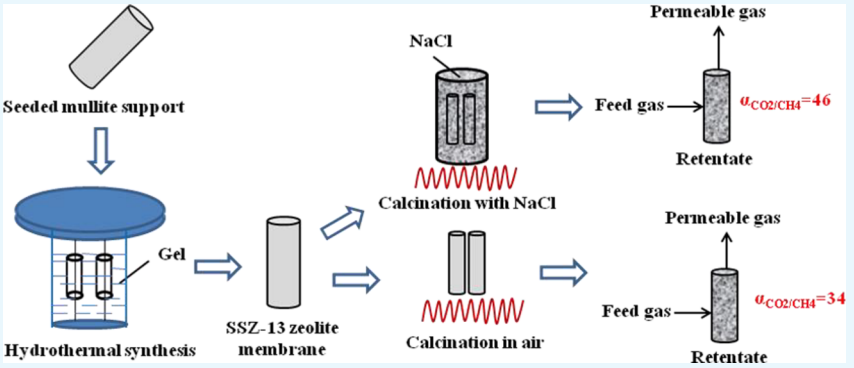

ABSTRACT: Hydrothermal synthesis with an organic template of *N,N,N* trimethyl-1-adamantammonium hydroxide (TMAdaOH) is the most commonly used method to prepare an SSZ-13 zeolite membrane. In this paper, the synthesized membrane was treated in heated sodium chloride to remove TMAdaOH instead of calcination in air. The surface of the membrane was modified by the heated NaCl and resulted in an improved CO_2/CH_4 gas separation selectivity. $TMAda^+$ in the channels of SSZ-13 zeolite decomposed completely, and the treatment time was shortened significantly compared with calcination in air. The recrystallization of zeolite reacting with heated NaCl was the possible reason for the improved gas separation performance of the membrane.

1. INTRODUCTION

Membrane technology has attracted increasing attention for biogas purification as an energy-saving and green method. Several types of zeolite membranes, including MFI,[1] DDR,[2] CHA,[3,4] AEI,[5] and ERI,[6] were reported to separate CO_2/CH_4 mixtures for molecular-sized pores and high mechanical, thermal, and chemical stabilities.

The CHA topological zeolite SSZ-13 has a three-dimensional structure with 8-membered pores of 0.38 nm and was reported to have high adsorption selectivity of CO_2 over N_2 and CH_4.[7] SSZ-13 zeolite membranes were prepared by in situ crystallization,[8] hydrothermal secondary growth,[9−14] inter-zeolite conversion,[15−17] and so forth, among which hydrothermal secondary growth was the most widely used method for controlling nucleation and crystal growth easily.

Organic template of *N,N,N*-trimethyl-1-adamantammonium hydroxide (TMAdaOH) was essential for the preparation of an SSZ-13 zeolite membrane by hydrothermal secondary growth. Chen et al.[12,18] investigated the $TMAdaOH/SiO_2$ ratio in gel and optimized the synthesis conditions. TMAdaOH must be removed before gas separation test for blocking the channels of SSZ-13 zeolite. The traditional way to remove TMAdaOH from the membrane was calcination at 550 °C in air for about 10 h,[10,13,14] which resulted in defects for mismatch of the thermal expansion coefficient between the membrane and the support. An improved way to reduce defects was calcination in oxygen[19,20] or pretreatment with ozonication,[21,22] but it needed more investment in equipment. Rapid thermal processing has been reported recently to avoid the formation of defects.[23] The membranes were placed in a quartz tube under vacuum and moved fast into a preheated oven at 1000 °C,[24] but the operation process was complex.

The defect generated in the preparation and calcination of the membrane was typically nonselective for gas separation, and several defect-patching methods were suggested. By deposition of methyldiethoxysilane,[25] tetraethylorthosilicate,[26] siloxane,[27] amorphous silica,[28] dye molecules,[29] or ionic liquids[30] on the surface of the membrane, the gas separation selectivity was improved successfully. However, the deposition

Received: November 4, 2021
Accepted: February 7, 2022
Published: February 17, 2022

https://doi.org/10.1021/acsomega.1c06215
ACS Omega 2022, 7, 6721−6727

layer was not a porous material, which resulted in the decrease in permeance notably, and the defects in the membrane remained. Another strategy is prompting the recrystallization of zeolite on the surface of the membrane to heal the defects. Molten salt method was widely used in the metal-processing field as a surface treatment technology with the advantages of heating evenly and no overheating.[31,32] However, the over-high temperature above the melting point of salt threatens the zeolite framework. In this paper, SSZ-13 zeolite membrane was treated in heated NaCl at temperatures varying from 500 to 550 °C to remove TMAdaOH, and the surface of the membrane was modified, too. The gas separation test showed that the membrane had an improved gas separation performance.

2. RESULTS AND DISCUSSION

2.1. Template Removal from the Membrane with Heated NaCl. SSZ-13 zeolite membranes were prepared with the initial gel composition of 1.0 SiO_2/0.005 Al_2O_3/0.10 Na_2O/0.10 TMAdaOH/80 H_2O and crystallized at 160 °C for 48 h. The membrane after hydrothermal synthesis had no gas separation performance because $TMAda^+$ occupied the channels of zeolite.[24] The traditional way to remove $TMAda^+$ was calcination in air at 550 °C for 10 h with heating and cooling rates of 0.25 °C/min, which takes a long time of about 3 days to avoid cracks.

In this paper, the synthesized SSZ-13 zeolite membrane was calcined in NaCl to remove TMAdaOH with the heating rate speeded up to reduce the time. The calcination time was shortened by using heated NaCl due to the difference in the specific heat capacity (SHC) between salt and air. The SHC of NaCl is 4.03 kJ/(kg °C) and that of air is 1.005 kJ/(kg °C) at 27 °C. Thus, salt could endure the temperature fluctuation better than air even at a high heating rate. As the decomposition temperature of TMAdaOH ranged from 420 to 600 °C, the temperature of NaCl was varied from 500 to 550 °C. At this temperature, NaCl was kept in the solid state. The membrane layer came in contact with air through the space between salt particles.

Figure 1 shows the X-ray diffraction (XRD) patterns of fresh SSZ-13 zeolite membranes treated in air and in NaCl. All membranes correspond to CHA structure reported by zones.[33] The membranes treated with salt (Figure 1b–d) had typical CHA peaks and higher crystallinity than the one (Figure 1a) calcined in air. However, the membranes treated with 500 °C/6 h and 550 °C/4 h were pale yellow, showing that the organic template was removed incompletely.

To investigate the mechanism of template removal with heated NaCl, uncalcined SSZ-13 zeolites, those calcined in air at 550 °C for 10 h, and those calcined in heated NaCl at 550 °C for 6 h were characterized with XRD, as shown in Figure 2. All the samples retained the CHA structure. The positions of the strongest peak in XRD patterns changed from 20.87 to 9.62 of 2θ after calcination in air or in salt compared to the fresh membrane, which resulted from the preferred orientation of planes in a lattice change from $[20\bar{1}]$ to $[100]$.[33,34] It was noticed that a weak peak appeared at 2θ of the 6.52 position in the XRD pattern of uncalcined SSZ-13 zeolite and those calcined in NaCl but disappeared after calcination in air, which was due to the flexibility of the rhombohedral lattice of SSZ-13 zeolite.

Thermogravimetric analysis (TGA) was applied to investigate the weight loss of fresh SSZ-13 zeolite and the one

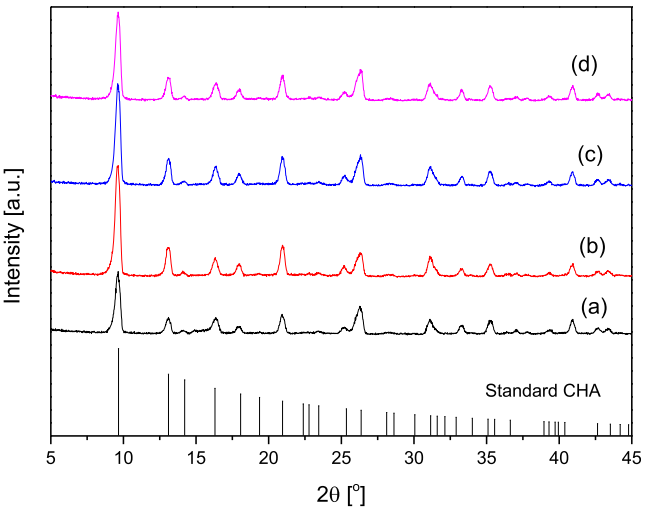

Figure 1. XRD patterns of SSZ-13 zeolite membranes calcined (a) in air at 550 °C/10 h and in heated NaCl at (b) 500 °C/6 h, (c) 550 °C/6 h, and (d) 550 °C/4 h.

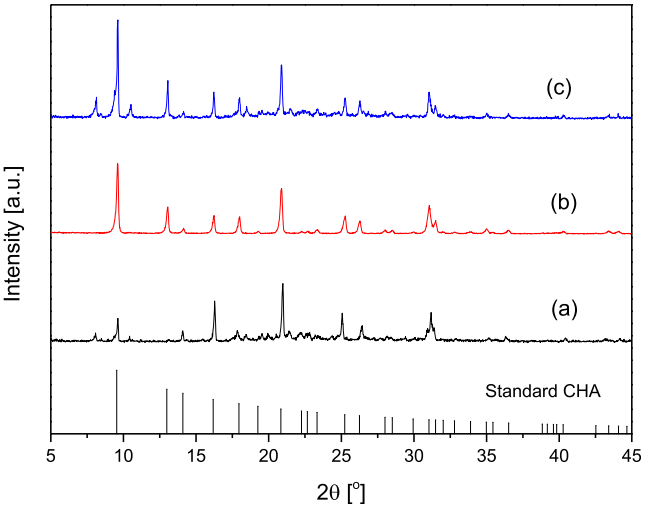

Figure 2. XRD patterns of (a) uncalcined SSZ-13 zeolite, (b) SSZ-13 zeolite calcined in air at 550 °C for 10 h, and (c) SSZ-13 zeolite calcined in heated NaCl at 550 °C for 6 h.

calcined in sodium chloride at various temperatures. Figure 3a shows the TGA curve of fresh SSZ-13 zeolite at a heating rate of 5 °C/min without an intermediate dwell time, indicating that the weight loss mainly occurred from 420 to 600 °C. TMAdaOH was removed effectively at 480,[5] 500 °C[12] in air, or 450 °C in pure oxygen,[6] and SSZ-13 zeolite membranes were reported with excellent gas separation performance. Figure 3b shows that the weight of SSZ-13 zeolite remained stable after calcination in heated NaCl at 550 °C for 6 h, indicating that the organic template in channels decomposed completely.

Adsorption isotherms for N_2 on SSZ-13 zeolite calcined in air at 550 °C for 10 h and in heated NaCl at 550 °C for 6 h are shown as Figure 4. The absorption amount for N_2 on SSZ-13 zeolite calcined in NaCl was higher than that on zeolite calcined in air. The Brunauer–Emmett–Teller (BET) SSA of SSZ-13 zeolite calcined in air is 492 m^2/g, which is higher than the BET SSA of SSZ-13 zeolite calcined in NaCl (420 m^2/g). The pore size distributions of SSZ-13 zeolite calcined in air and in heated NaCl are shown in Figure S1. The pore size

https://doi.org/10.1021/acsomega.1c06215
ACS Omega 2022, 7, 6721−6727

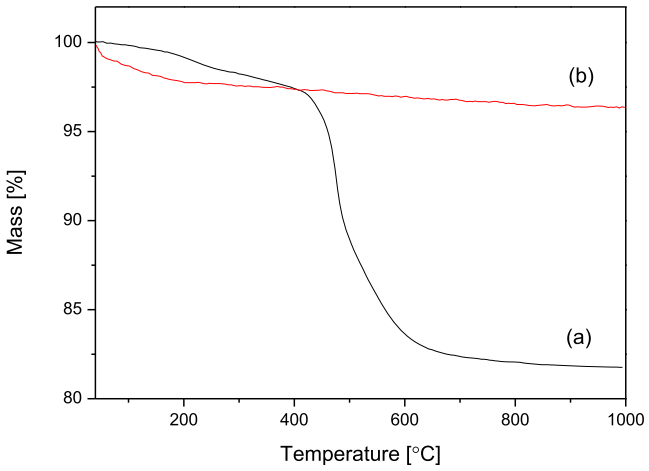

Figure 3. TGA of (a) uncalcined SSZ-13 zeolite and (b) SSZ-13 zeolite calcined with NaCl at 550 °C for 6 h.

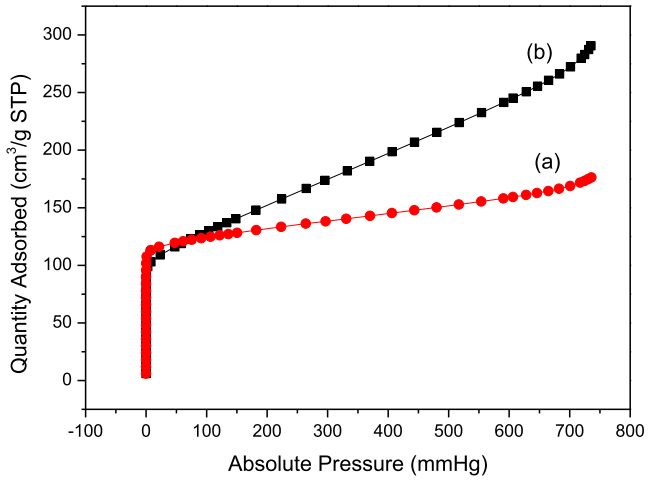

Figure 4. Adsorption isotherms for N_2 on SSZ-13 zeolite calcined (a) in air at 550 °C for 10 h and (b) in heated NaCl at 550 °C for 6 h.

distributions of SSZ-13 zeolites were close between the two calcinations ways.

TMAdaOH reacted with oxygen and decomposed to N_2, H_2O, and CO_2 when SSZ-13 zeolite was calcined in air at 550 °C for 10 h, which escaped from the channels easily. During the calcination with NaCl at 550 °C for 6 h, oxygen entered from the spaces between salt particles and reacted with TMAdaOH, which might decompose to carbon, similar to the process of carbon film preparation.[35−37] The CO_2/CH_4 ideal selectivity of the membrane treated with NaCl was improved maybe due to the blocking of pinhole defects with the produced carbon. In order to verify the hypothesis and investigate the change in functional groups after heated salt treatment, Fourier transform infrared spectrometry (FTIR) was carried out for SSZ-13 zeolite, as shown in Figure 5. The IR spectrum peaks corresponding to the functional groups are shown in Table 1.[38] After calcination in air or in heated salt, the peaks corresponding to functional groups of $-CH_3$, $-CH_2$, and N−H disappeared, indicating that TMAdaOH decomposed completely and no carbon was produced.

To verify whether carbon existed in the channels of SSZ-13 zeolite produced from the decomposition of TMAdaOH, Raman spectrum characterization was performed. Figure 6 shows the Raman spectrum of SSZ-13 zeolite calcined in air at

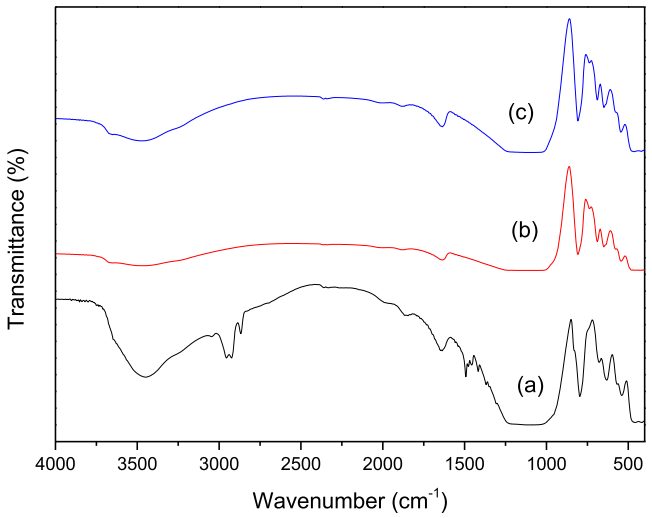

Figure 5. FTIR of (a) uncalcined SSZ-13 zeolite, (b) SSZ-13 zeolite calcined in air at 550 °C for 10 h, and (c) SSZ-13 zeolite calcined in heated NaCl at 550 °C for 6 h.

Table 1. FTIR Spectra Peaks Corresponding to Functional Groups

no.	wavenumber/cm^{-1}	the corresponding functional groups
1	3440	N−H stretching vibration
2	2900−2850	$-CH_2$ bending vibration
3	2850−2750	$-CH_3$ stretching vibration
4	1630	N−H bending vibration
5	1450−1350	$-CH_3$ bending vibration
6	1300−1000	C−N vibration
7	1240−1060	O−Si−O or O−Al−O asymmetric bending vibration
8	790	Al−O symmetric vibration
9	650−580	double 6-member vibration
10	420	Si−O or Al−O tetrahedral bending vibration

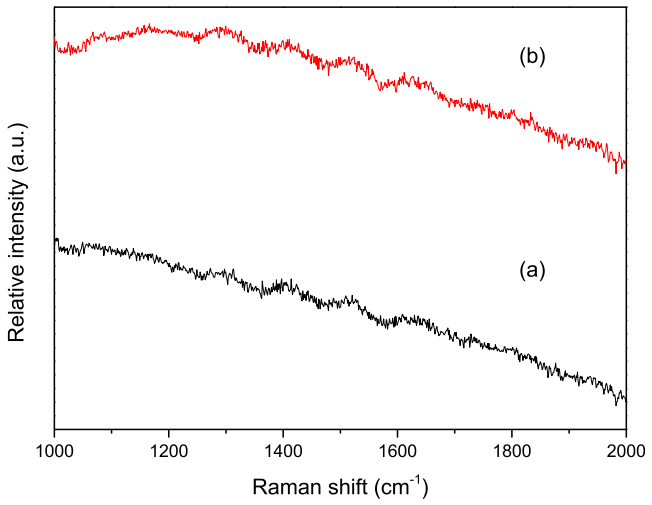

Figure 6. Raman spectrum of SSZ-13 zeolite (a) calcined in air at 550 °C for 10 h and (b) treated with heated NaCl at 550 °C for 6 h.

550 °C for 10 h and in heated NaCl at 550 °C for 6 h. The Raman shift corresponds to natural graphite at 1580 cm^{-1} as G-line; at 1345 cm^{-1} as D-line; low-order structures at 1180, 1500, and 1620 cm^{-1}; and so forth.[39] However, no typical peaks corresponding to carbon appeared. In addition, energy-

https://doi.org/10.1021/acsomega.1c06215
ACS Omega 2022, 7, 6721−6727

dispersive X-ray spectroscopy (EDS) of SSZ-13 zeolite was carried out, and the results showed that almost no carbon existed on the surface of zeolite after the treatment with heated salt. As a result, TMAdaOH decomposed completely and no carbon was produced in the channels of SSZ-13 zeolite after treatment with heated NaCl.

2.2. Surface Modification of the Membrane with Heated NaCl. Figure 7 shows the surface and cross-sectional

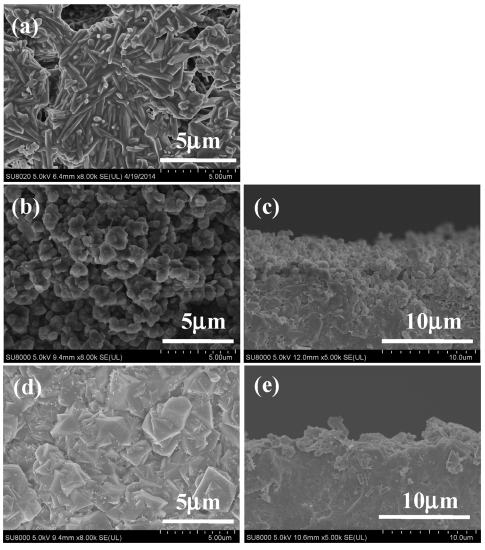

Figure 7. SEM images of the (a) surface of mullite support and the surface and cross section of the SSZ-13 zeolite membrane calcined in air (b,c) at 550 °C for 10 h and in heated NaCl (d,e) at 550 °C for 6 h.

SEM images of the SSZ-13 zeolite membrane treated with heated NaCl at 550 °C for 6 h. Compared to the membrane calcined in air at 550 °C for 10 h (Figure 7b,c), the surface of the SSZ-13 membrane treated with heated salt shows a dense and good intergrowth layer (Figure 7d), and the membrane layer integrated with the support (Figure 7e). Although some salts infected the surface of the membrane, an improved CO_2/CH_4 selectivity was obtained. The membrane treated with heated sodium chloride was characterized by EDS, and the sodium chloride had only 3.88 wt %.

To investigate the surface modification with heated salt, SSZ-13 zeolite was used. The conventional morphology of the synthesized SSZ-13 zeolite was rhombohedral and spherical, as shown in Figure 8a. A crystal with complete crystallization showed rhombohedral morphology, and the spherical morphology came from the stacking of crystals. The rhombohedral and spherical morphologies coexisted when SSZ-13 zeolite was calcined in air, which was reported in our previous work.[10] However, only rhombohedral crystals were

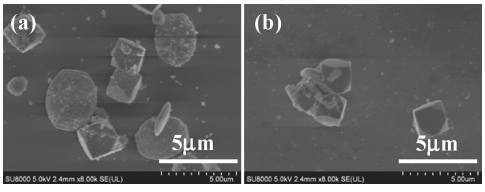

Figure 8. SEM images of (a) uncalcined SSZ-13 zeolite and (b) SSZ-13 zeolite treated with heated NaCl at 550 °C for 6 h.

observed when SSZ-13 zeolite was treated with heated salt, as shown in Figure 8b, and the spherical crystals were not observe maybe due to recrystallization.

No recrystallization behavior of SSZ-13 zeolite crystals was observed when calcined in air, why it occurred in heated salt? Recrystallization of conventional coarse-grained metals was investigated, and Hibbard et al.[40] reported nanocrystalline nickle recrystallized and grown by isothermal annealing. Reber et al.[41] reported coarse-grained silicon films on SiAlON ceramics recrystallized by zone melting. Guzmán-Castillo et al.[42] reported that Y zeolite was depolymerized with glycerol at 200 and 250 °C and partially recrystallized in the presence of either a structure-directing agent (CTAB) or ammonium ions (NH_4NO_3/NH_4OH). However, there is no report on the recrystallization of zeolite with heated salt, but it is the most possible explanation for the improved gas separation performance of the SSZ-13 zeolite membrane. SSZ-13 zeolite was recrystallized in the treatment of heated salt, and the spherical morphology transformed to a rhombohedral morphology after salt treatment, as shown in Figure 8b, was an obvious proof. This supplied a novel way to control the quality of SSZ-13 zeolite and its membrane with no defect.

2.3. Gas Separation Performance of the Membrane Treated in Heated Salt. SSZ-13 membranes were prepared repeatedly with secondary hydrothermal growth, and the high performance of the membrane calcined in air had a CO_2 permeance of 3.21×10^{-7} mol/(m²·s·Pa) and CO_2/CH_4 selectivity of 34. The gas separation performances of SSZ-13 zeolite membranes treated in air and with heated salt are shown as Table 2; the membranes were tested at 25 °C and the

Table 2. Single Gas Separation Performance of SSZ-13 Zeolite Membranes Treated in Air and in Heated NaCl

no.	treatment methods	conditions	CO_2 permeance [$\times 10^{-7}$ mol/(m²·s·Pa)]	ideal selectivity of CO_2/CH_4
1	calcination in air	550 °C/10 h	3.21	34
2	in heated NaCl	500 °C/6 h	1.82	58
3	in heated NaCl	550 °C/6 h	2.01	46
4	in heated NaCl	550 °C/4 h	1.80	49

feed gas pressure was 0.4 MPa. TMAdaOH was removed effectively from the SSZ-13 zeolite membrane with heated salt treatment at 550 °C/6 h, and the membrane had a CO_2 permeance of 2.01×10^{-7} mol/(m²·s·Pa) and CO_2/CH_4 selectivity of 46. TMAdaOH occupying the channels of the SSZ-13 zeolite membrane was removed incompletely at 500 °C/6 h and 550 °C/4 h, which induced lower CO_2 permeance but higher CO_2/CH_4 selectivity. All the membranes treated with heated salt had higher CO_2/CH_4 selectivities compared to the membranes calcined in air, and the membrane treated at 500 °C/6 h had an improved CO_2/CH_4 selectivity of 71% than the one calcined in air.

3. CONCLUSIONS

A novel method of heated NaCl treatment was used to remove the organic template of TMAdaOH from the channels of the SSZ-13 zeolite membrane instead of conventional calcination in air. The membrane generated less cracks by heated salt

https://doi.org/10.1021/acsomega.1c06215
ACS Omega 2022, 7, 6721−6727

treatment, and the required time for template removal was reduced significantly. Besides, the treatment could be carried out in a normal muffle furnace. $TMAda^+$ in the channels of SSZ-13 zeolite decomposed completely, which reacted with oxygen that entered from the space between salt particles. The SSZ-13 zeolite membrane treated with heated NaCl had an improved gas separation performance, and the possible reason was the recrystallization of zeolite crystals after the heated salt treatment, which changed the morphology of crystals from spherical to rhombohedral. The optimized condition for the heated salt treatment was 550 °C for 6 h, and the membrane had a CO_2 permeance of 2.01 × 10^{-7} mol/(m^2·s·Pa) and a CO_2/CH_4 selectivity of 46.

4. EXPERIMENTAL SECTION

4.1. Membrane Fabrication and Treatment. SSZ-13 zeolite and membranes were synthesized and introduced in our previous work.[10,12,18] The SSZ-13 zeolite membrane was synthesized on porous mullite tubes (length: 10 cm, outside diameter: 12 mm, inner diameter: 9 mm, thickness: 1.5 mm, average pore size: 1.3 μm, porosity: 30−40%, Nikkato Corp., Tokyo, Japan) by secondary hydrothermal synthesis. The synthesis gel with a molar ratio of 1.0 SiO_2/0.005 Al_2O_3/0.1 Na_2O/0.1 TMAdaOH/80 H_2O was mixed with NaOH (96%, Junzheng, Wuhai, China), TMAdaOH (25%, Ankai, Tokyo, Japan), $Al(OH)_3$ (99%, Wako, Tokyo, Japan), deionized (DI) water (homemade), and colloidal silica (Ludox TM-40, Sigma-Aldrich, St. Louis, MO, USA). After synthesis, the membranes were washed with running tap water, soaked in DI water until neutral, and dried in a conventional oven. Sodium chloride (AR, 99.5%, Sinopharm, Shanghai, China) was filled in a corundum crucible with two vertically placed SSZ-13 membranes at 550 °C for 6 h without controlling the heating rate for template removal and surface modification, as shown in Figure 9. There was no pretreatment of sodium chloride. The particle size of NaCl was less than 0.15 mm and the purity was ≥99.5%. As a comparison, the traditional way to remove TMAdaOH was calcined in air at 550 °C for 10 h with heating and cooling rate of 0.25 °C/min. After treatment, the membranes were stored in a conventional oven at 100 °C before characterization and gas separation test.

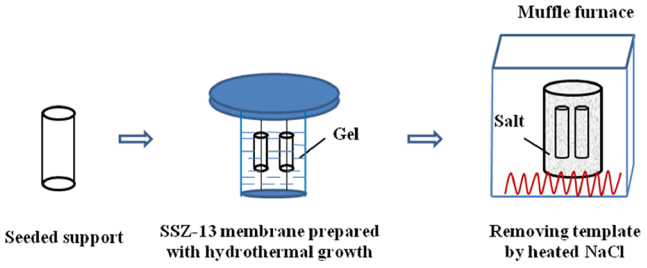

Figure 9. Schematic diagram for the procedure of template removal and surface modification of the SSZ-13 zeolite membrane by heated NaCl.

4.2. Characterization. The thermal weight loss of samples was analyzed using TGA (NETZSCH STA 449F3, USA), and the carrier gas was a mixture of N_2 (80%) and O_2 (20%), with a heating rate of 5 °C/min, initial temperature of 40 °C, and the finial temperature of 1000 °C. The sample weight was 5 ± 0.5 mg.

SSZ-13 zeolites and membranes were identified by XRD (Rigaku Ultima IV, Japan) using Cu Kα radiation (λ = 0.15406 nm), and the operating conditions were 40 kV and 40 mA in air with 2θ at 5−45° and a step size of 0.02°. Relative crystallinity was estimated by comparing the sum of typical peak intensities (at 2θ = 9.6, 12.9, and 20.6°) of the samples, with the membrane having the highest crystallinity as identified by XRD.

The morphologies of samples were observed with a field emission scanning electron microscope (Hitachi SU8020, Japan) at acceleration voltages from 3 to 10 kV. To improve the conductivity and obtain clear SEM images, the samples of zeolite and membranes were coated with Pt before SEM characterization. EDS (Bruker Q200, USA) was used to identify the elemental composition.

FTIR (Bruker Tensor II, USA) was used in the wavenumber range of 400−4000 cm^{-1}, and the concentration of samples in the KBr pellets was 1%, which was accumulated with 256 scans to obtain the IR spectra.

Raman spectrum measurements were taken with a laser Raman spectrometer (LabRAM HR Jobin Yvon, France), and the excitation wavelength was 632.8 nm. The focal length of the spectrometer was 800 mm, and the scanning frequency shift range was 200−2000 cm^{-1}.

Nitrogen adsorption isotherms were measured at −196 °C using a volumetric adsorption analyzer (Micromeritics ASAP2460, USA), with samples being degassed at 300 °C under vacuum. The BET model surface area (S_{BET}), total pore volume (V_{total}), and micropore volume (V_{micro}) were calculated from the nitrogen isotherms.

Single-gas permeation of SSZ-13 membranes was tested with a dead-end and retentate stream blocked system without sweep gas according to our previous study.[12,18] The permeate flow rates of CO_2 and CH_4 were measured with a soap bubble flowmeter, and the ideal selectivity of the membrane was the ratio of two single-gas permeances with each data point obtained at the stabilization status.

The permeance (P_i) is calculated by eq 1

$$P_i = N_i/(A \cdot \Delta P) \quad (1)$$

where N_i (mol/s) is the membrane flux of component i, A (m^2) is the effective surface area of the SSZ-13 zeolite membrane, and ΔP (Pa) is the pressure drop across the membrane. The ideal selectivity (S) for CO_2/CH_4 is calculated by eq 2

$$S = P_{CO_2}/P_{CH_4} \quad (2)$$

.

■ ASSOCIATED CONTENT

Supporting Information

The Supporting Information is available free of charge at https://pubs.acs.org/doi/10.1021/acsomega.1c06215.

Pore size distribution of SSZ-13 zeolite calcined in air at 550 °C for 10 h and in heated NaCl at 550 °C for 6 h (PDF)

■ AUTHOR INFORMATION

Corresponding Author

Xiang-Shu Chen − *Institute of Advanced Materials, State-Province Joint Engineering Laboratory of Zeolite Membrane Materials, College of Chemistry and Chemical Engineering,*

https://doi.org/10.1021/acsomega.1c06215
ACS Omega 2022, 7, 6721−6727

Jiangxi Normal University, Nanchang 330022, P. R. China; orcid.org/0000-0003-2378-2271; Phone: +86-25-8812-0533; Email: cxs66cn@jxnu.edu.cn

Authors

He-Li Wang − *Institute of Advanced Materials, State-Province Joint Engineering Laboratory of Zeolite Membrane Materials, College of Chemistry and Chemical Engineering, Jiangxi Normal University, Nanchang 330022, P. R. China; Energy Institute, Jiangxi Academy of Sciences, Nanchang 330096, P. R. China*

Mei-Hua Zhu − *Institute of Advanced Materials, State-Province Joint Engineering Laboratory of Zeolite Membrane Materials, College of Chemistry and Chemical Engineering, Jiangxi Normal University, Nanchang 330022, P. R. China;* orcid.org/0000-0003-2496-080X

Ting Wu − *Institute of Advanced Materials, State-Province Joint Engineering Laboratory of Zeolite Membrane Materials, College of Chemistry and Chemical Engineering, Jiangxi Normal University, Nanchang 330022, P. R. China*

Qin-Liang Jiang − *Energy Institute, Jiangxi Academy of Sciences, Nanchang 330096, P. R. China*

Fei Zhang − *Institute of Advanced Materials, State-Province Joint Engineering Laboratory of Zeolite Membrane Materials, College of Chemistry and Chemical Engineering, Jiangxi Normal University, Nanchang 330022, P. R. China*

Ya-Fen Wu − *Research Department, Jiangxi University of Traditional Chinese Medicine, Nanchang 330004, P. R. China*

Complete contact information is available at: https://pubs.acs.org/10.1021/acsomega.1c06215

Notes

The authors declare no competing financial interest.

■ ACKNOWLEDGMENTS

We gratefully acknowledge the financial support to this work from the National Natural Science Foundation of China (grant nos. 21968009, 21868012, and 21766010), the International Science and Technology Cooperation Program of China (grant no. 2015DFA50190), and the Jiangxi Provincial Department of Science and Technology (grant no. 20171BCB24005).

■ REFERENCES

(1) Sandström, L.; Sjöberg, E.; Hedlund, J. Very high flux MFI membrane for CO_2 separation. *J. Membr. Sci.* **2011**, *380*, 232−240.

(2) Tomita, T.; Nakayama, K.; Sakai, H. Gas separation characteristics of DDR type zeolite membrane. *Microporous Mesoporous Mater.* **2004**, *68*, 71−75.

(3) Kalipcilar, H.; Bowen, T. C.; Noble, R. D.; Falconer, J. L. Synthesis and separation performance of SSZ-13 zeolite membranes on tubular supports. *Chem. Mater.* **2002**, *14*, 3458−3464.

(4) Kosinov, N.; Auffret, C.; Gücüyener, C.; Szyja, B. M.; Gascon, J.; Kapteijn, F.; Hensen, E. J. M. High flux high-silica SSZ-13 membrane for CO_2 separation. *J. Mater. Chem. A* **2014**, *2*, 13083−13092.

(5) Wu, T.; Wang, B.; Lu, Z.; Zhou, R.; Chen, X. Alumina-supported AlPO-18 membranes for CO_2/CH_4 separation. *J. Membr. Sci.* **2014**, *471*, 338−346.

(6) Zhong, S.; Bu, N.; Zhou, R.; Jin, W.; Yu, M.; Li, S. Aluminophosphate-17 and silicoaluminophosphate-17 membranes for CO_2 separations. *J. Membr. Sci.* **2016**, *520*, 507−514.

(7) Maghsoudi, H.; Soltanieh, M.; Bozorgzadeh, H.; Mohamadalizadeh, A. Adsorption isotherms and ideal selectivities of hydrogen sulfide and carbon dioxide over methane for the Si-CHA zeolite: comparison of carbon dioxide and methane adsorption with the all-silica DD3R zeolite. *Adsorption* **2013**, *19*, 1045−1053.

(8) Maghsoudi, H.; Soltanieh, M. Simultaneous separation of H_2S and CO_2 from CH_4 by a high silica CHA-type zeolite membrane. *J. Membr. Sci.* **2014**, *470*, 159−165.

(9) Sun, C.; Srivastava, D. J.; Grandinetti, P. J.; Dutta, P. K. Synthesis of Chabazite/polymer composite membrane for CO_2/N_2 separation. *Microporous Mesoporous Mater.* **2016**, *230*, 208−216.

(10) Zheng, Y.; Hu, N.; Wang, H.; Bu, N.; Zhang, F.; Zhou, R. Preparation of stream-stable high-silica CHA (SSZ-13) membranes for CO_2/CH_4 and C_2H_4/C_2H_6 separation. *J. Membr. Sci.* **2015**, *475*, 303−310.

(11) Kosinov, N.; Auffret, C.; Borghuis, G. J.; Sripathi, V. G. P.; Hensen, E. J. M. Influence of the Si/Al ratio on the separation properties of SSZ-13 zeolite membranes. *J. Membr. Sci.* **2015**, *484*, 140−145.

(12) Liang, L.; Zhu, M.; Chen, L.; Zhong, C.; Yang, Y.; Wu, T.; Wang, H.; Kumakiri, I.; Chen, X.; Kita, H. Single Gas Permeance Performance of High Silica SSZ-13 Zeolite Membranes. *Membranes* **2018**, *8*, 43.

(13) Kida, K.; Maeta, Y.; Yogo, K. Preparation and gas permeation properties on pure silica CHA-type zeolite membranes. *J. Membr. Sci.* **2017**, *522*, 363−370.

(14) Kida, K.; Maeta, Y.; Yogo, K. Pure silica CHA-type zeolite membranes for dry and humidified CO_2 /CH_4 mixtures separation. *Sep. Purif. Technol.* **2018**, *197*, 116−121.

(15) Itakura, M.; Goto, I.; Takahashi, A.; Fujitani, T.; Ide, Y.; Sadakane, M.; Sano, T. Synthesis of high-silica CHA type zeolite by interzeolite conversion of FAU type zeolite in the presence of seed crystals. *Microporous Mesoporous Mater.* **2011**, *144*, 91−96.

(16) Zones, S. I. Direct hydrothermal conversion of cubic P zeolite to organozeolite SSZ-13. *J. Chem. Soc., Faraday Trans.* **1990**, *86*, 3467−3472.

(17) Geng, H.; Li, G.; Liu, D.; Liu, C. Rapid and efficient synthesis of CHA-type zeolite by interzeolite conversion of LTA-type zeolite in the presence of N, N, N-trimethyladamantammonium hydroxide. *J. Solid State Chem.* **2018**, *265*, 193−199.

(18) Zhu, M.; Liang, L.; Wang, H.; Liu, Y.; Wu, T.; Zhang, F.; Li, Y.; Kumakiri, I.; Chen, X.; Kita, H. Influences of Acid Post-Treatment on high silica SSZ-13 zeolite membrane. *Ind. Eng. Chem. Res.* **2019**, *58*, 14037−14043.

(19) Wang, B.; Zheng, Y.; Zhang, J.; Zhang, W.; Zhang, F.; Xing, W.; Zhou, R. Separation of light gas mixtures using zeolite SSZ-13 membranes. *Microporous Mesoporous Mater.* **2019**, *275*, 191−199.

(20) Song, S.; Gao, F.; Zhang, Y.; Li, X.; Zhou, M.; Wang, B.; Zhou, R. Preparation of SSZ-13 membranes with enhanced fluxes using asymmetric alumina supports for N_2/CH_4 and CO_2/CH_4 separations. *Sep. Purif. Technol.* **2019**, *209*, 946−954.

(21) Kosinov, N.; Auffret, C.; Sripathi, V. G. P.; Gücüyener, C.; Gascon, J.; Kapteijn, F.; Hensen, E. J. M. Influence of support morphology on the detemplation and permeation of ZSM-5 and SSZ-13 zeolite membranes. *Microporous Mesoporous Mater.* **2014**, *197*, 268−277.

(22) Karakiliç, P.; Wang, X.; Kapteijn, F.; Nijmeijer, A.; Winnubst, L. Defect-free high-silica CHA zeolite membranes with high selectivity for light gas separation. *J. Membr. Sci.* **2019**, *586*, 34−43.

(23) Chang, N.; Tang, H.; Bai, L.; Zhang, Y.; Zeng, G. Optimized rapid thermal processing for the template removal of SAPO-34 zeolite membranes. *J. Membr. Sci.* **2018**, *552*, 13−21.

(24) Kim, J.; Jang, E.; Hong, S.; Kim, D.; Kim, E.; Richter, H.; Simon, A.; Choi, N.; Korelskiy, D.; Fouladvand, S.; Nam, J.; Choi, J. Microstructural control of a SSZ-13 zeolite film via rapid thermal processing. *J. Membr. Sci.* **2019**, *591*, 117342.

(25) Hong, M.; Falconer, J. L.; Noble, R. D. Modification of zeolite membranes for H_2 separation by catalytic cracking of methyldiethoxysilane. *Ind. Eng. Chem. Res.* **2005**, *44*, 4035−4041.

(26) Kanezashi, M.; O'Brien-Abraham, J.; Lin, Y. S.; Suzuki, K. Gas permeation through DDR-type zeolite membranes at high temperatures. *AIChE J.* **2008**, *54*, 1478−1486.

(27) Zhou, R.; Wang, H.; Wang, B.; Chen, X.; Li, S.; Yu, M. Defect-patching of zeolite membranes by surface modification using siloxane polymers for CO_2 separation. *Ind. Eng. Chem. Res.* **2015**, *54*, 7516−7523.
(28) Karimi, S.; Korelskiy, D.; Yu, L.; Mouzon, J.; Khodadadi, A. A.; Mortazavi, Y.; Esmaeili, M.; Hedlund, J. A simple method for blocking defects in zeolite membranes. *J. Membr. Sci.* **2015**, *489*, 270−274.
(29) Hong, S.; Kim, D.; Jeong, Y.; Kim, E.; Jung, J. C.; Choi, N.; Nam, J.; Yip, A. C. K.; Choi, J. Healing of microdefects in SSZ-13 membranes via filling with dye molecules and its effect on dry and wet CO_2 separations. *Chem. Mater.* **2018**, *30*, 3346−3358.
(30) Liu, B.; Zhou, R.; Bu, N.; Wang, Q.; Zhong, S.; Wang, B.; Hidetoshi, K. Room-temperature ionic liquids modified zeolite SSZ-13 membranes for CO2/CH4 separation. *J. Membr. Sci.* **2017**, *524*, 12−19.
(31) Yeung, C. F.; Lau, K. H.; Li, H. Y.; Luo, D. F. Advanced QPQ complex salt bath heat treatment. *J. Mater. Process. Technol.* **1997**, *66*, 249−252.
(32) Peng, T.; Dai, M.; Cai, W.; Wei, W.; Wei, K.; Hu, J. The enhancement effect of salt bath preoxidation on salt bath nitriding for AISI 1045 steel. *Appl. Surf. Sci.* **2019**, *484*, 610−615.
(33) Zones, S. I. Zeolite SSZ-13 and its method of preparation. U.S. Patent 4,544,538 A, Oct 01, 1985.
(34) Treacy, M. M. J.; Higgins, J. B. *Collection of Simulated XRD Powder Patterns for Zeolites*, 4th ed.; Elsevier: Amsterdam, 2001; p 102.
(35) Barsema, J.; Klijnstra, S.; Balster, J.; van der Vegt, N.; Koops, G.; Wessling, M. Intermediate polymer to carbon gas separation membranes based on Matrimid PI. *J. Membr. Sci.* **2004**, *238*, 93−102.
(36) Sazali, N.; Salleh, W. N. W.; Ismail, A. F.; Kadirgama, K.; Othman, F. E. C.; Ismail, N. H. Impact of stabilization environment and heating rates on P84 co-polyimide/nanocrystaline cellulose carbon membrane for hydrogen enrichment. *Int. J. Hydrogen Energy* **2019**, *44*, 20924−20932.
(37) Yoshimune, M.; Haraya, K. Simple control of the pore structures and gas separation performances of carbon hollow fiber membranes by chemical vapor deposition of propylene. *Sep. Purif. Technol.* **2019**, *223*, 162−167.
(38) Tang, J.; Zhou, Y.; Su, W.; Liu, X.; Sun, Y. Synthesis of Zeolite SSZ-13 for N_2 and CO_2 Separation. *Adsorpt. Sci. Technol.* **2013**, *31*, 549−558.
(39) Hao, J.; Lyu, C.; Li, D. Characterization of the microstructure of carbon fibers: Raman spectroscopy. *Chem. Ind. Eng. Prog.* **2020**, *39*, 227−233.
(40) Hibbard, G. D.; Radmilovic, V.; Aust, K. T.; Erb, U. Grain boundary migration during abnormal grain growth in nanocrystalline Ni. *Mater. Sci. Eng., A* **2008**, *494*, 232−238.
(41) Reber, S.; Zimmermann, W.; Kieliba, T. Zone melting recrystallization of silicon films for crystalline silicon thin-film solar cells. *Sol. Energy Mater. Sol. Cells* **2001**, *65*, 409−416.
(42) Guzmán-Castillo, M. L.; Armendáriz-Herrera, H.; Pérez-Romo, P.; Hernández-Beltrán, F.; Ibarra, S.; Valente, J. S.; Fripiat, J. J. Y zeolite depolymerization−recrystallization: Simultaneous formation of hierarchical porosity and Na dislodging. *Microporous Mesoporous Mater.* **2011**, *143*, 375−382.

https://doi.org/10.1021/acsomega.1c06215
ACS Omega 2022, 7, 6721−6727